

Maternal insulin resistance causes oxidative stress and mitochondrial dysfunction in mouse oocytes

Xiang-Hong Ou^{1,2}, Sen Li¹, Zhen-Bo Wang¹, Mo Li¹, Song Quan², Fuqi Xing², Lei Guo¹, Shi-Bin Chao, Zijiang Chen³, Xing-Wei Liang¹, Yi Hou¹, Heide Schatten⁴, and Qing-Yuan Sun^{1,*}

¹State Key Laboratory of Reproductive Biology, Institute of Zoology, Chinese Academy of Sciences, #1 Beichen West Road, Beijing 100101, People's Republic of China ²Center of Reproductive Medicine, Department of Obstetrics and Gynecology, Nanfang Hospital, Southern Medical University, Guangzhou 510515, People's Republic of China ³Research Center for Reproductive Medicine, Shandong Provincial Hospital of Shandong University, Jinan 250021, People's Republic of China ⁴Department of Veterinary Pathobiology, University of Missouri, Columbia, MO 65211, USA

*Correspondence address. Tel: +86-10-64807050; Fax: +86-10-64807050; E-mail: sunqy@ioz.ac.cn or sunqyl@yahoo.com

Submitted on October 23, 2011; resubmitted on March 12, 2012; accepted on March 23, 2012

BACKGROUND: Insulin resistance (IR) and hyperinsulinemia compromise fertility in females and are well-recognized characteristics of anovulatory women with polycystic ovary syndrome. Patients with IR and hyperinsulinemia undergoing ovarian stimulation for IVF are at increased risks of impaired oocyte developmental competence, implantation failure and pregnancy loss. However, the precise underlying mechanism remains unknown.

METHODS: We investigated how IR impairs oocyte quality and early embryonic development by an insulin-resistant mouse model. Oocyte quality, fertilization and embryonic development were analyzed. Furthermore, oxidant stress products and mitochondrial function were evaluated by quantitative real-time PCR and immunofluorescence.

RESULTS: An imbalance between oxidants and antioxidants revealed by increased concentrations of reactive oxygen species, and a decreased concentration of glutathione (GSH) and a decreased GSH/GSSG ratio resulted in oxidative stress (OS) and impaired mitochondrial function in germinal vesicle (GV) and metaphase II (MII) oocytes of insulin-resistant mice. MII oocytes displayed a decrease in the ATP content and the mitochondrial DNA (mtDNA) copy number. In contrast, GV oocytes were characterized by a high ATP content concomitant with increased clustering of mitochondria and a high inner mitochondrial membrane potential. GV oocytes from insulin-resistant mice showed early stage apoptosis, and fewer MII oocytes could be retrieved from these mice and were of poor quality associated with decreased fertilization and an arrest of embryo development with increased fragmentation. Abnormal spindles and misaligned chromosomes of MII oocyte were significantly increased in IR and hyperinsulinemia mice compared with the control mice.

CONCLUSIONS: IR contributes to OS and disrupts mitochondrial function in mouse oocytes. This may impair the accurate transmission of mtDNA from one generation to the next. Therefore, our results suggest that OS and mitochondrial dysfunction are responsible for poor oocyte quality of insulin-resistant mice, and may provide novel targets to improve low fertility in females with IR.

Key words: insulin resistance / hyperinsulinemia / oxidative stress / mitochondria / mouse oocyte

Introduction

Insulin resistance (IR) and hyperinsulinemia impair female reproduction and play an important role in the pathogenesis of polycystic ovary syndrome (PCOS) leading to reduced fecundity and a significantly increased risk of type 2 diabetes (Dale *et al.*, 1998; Svendsen *et al.*, 2008). Obesity exacerbates hyperinsulinemia and IR (Homburg

2002), affects the oocyte and embryo quality (Igosheva *et al.*, 2010), and reduces conception (Lintsen *et al.*, 2005). Lower fertilization and implantation rates, and an increased risk of spontaneous pregnancy loss after IVF occur in insulin-resistant women with PCOS (Cano *et al.*, 1997). In addition, IR affects the developmental potential of human immature oocytes in PCOS patients, as indicated by impaired oocyte maturation, fewer fertilized oocytes and cleaved

embryos (Ludwig *et al.*, 1999; Kovacs and Wood, 2001; Vlaisavljevic *et al.*, 2009). Fecundity is impaired in insulin-resistant and obese mice regardless of PCOS (Brothers *et al.*, 2010). The intrinsic quality of oocytes is a key factor that determines female fertility. However, until now the precise cellular and molecular mechanisms by which IR affects the oocyte quality has remained unclear.

Insulin stimulates mitochondrial function and it is a major regulating factor of mitochondrial oxidative phosphorylation (Boirie, 2003). IR increases ROS formation and impairs mitochondrial function (Kim *et al.*, 2008). The insulin receptor and insulin signaling have been described in human and mouse oocytes (Samoto *et al.*, 1993; Acevedo *et al.*, 2007). Mitochondria are the main energy generators within the ooplasm and their activity is closely correlated with the oocyte quality. Dysfunctional mitochondria, such as those with structural, spatial and genetic abnormalities in the oocytes, lead to chromosomal misalignment during meiotic division, and reduce the quality and developmental potential of oocytes. Intracytoplasmic injection of functional mitochondria can overcome mitochondrial dysfunctions and inhibit oocyte fragmentation (Nagai *et al.*, 2004). In contrast, injection of abnormal mitochondria induces oocyte apoptosis (Perez *et al.*, 2007). Thus, in the present study, we hypothesized that mitochondrial dysfunction in oocytes is responsible for low fertility and the high miscarriage rate in hyperinsulinemic and insulin-resistant females. Mitochondria are major sites of ROS production (Chen *et al.*, 2003); persistent and elevated generation of ROS causes oxidative stress (OS) (Ihnat *et al.*, 2007). Maintaining redox homeostasis is important for the generation of high-quality gametes and embryos. On molecular levels, higher ROS can alter several redox pathways and may eventually lead to apoptosis in oocytes and embryos (Agarwal *et al.*, 2008). During folliculogenesis, important antioxidants such as glutathione (GSH) protect oocytes against toxic injury due to OS. Suppression of GSH synthesis leads to increased rates of antral follicle atresia in rats (Tsai-Turton *et al.*, 2007). GSH also regulates protein and DNA synthesis by altering the redox status, and participates in microtubule assembly (Deneke and Fanburg, 1989; Luderer *et al.*, 2001). Interactions between mitochondria and the cytoskeleton influence mitochondrial respiratory activity and inheritance as well as localization of mitochondria, ROS biogenesis and dissemination of mitochondrial apoptotic factors (Boldogh and Pon, 2007).

The present study employs an insulin-resistant and hyperinsulinemic mouse model to determine whether IR will affect oocyte quality and to explore the underlying mechanism. We found that IR contributed to OS and compromised mitochondrial function in germinal vesicle (GV) and metaphase II (MII) oocytes.

Materials and Methods

All chemicals and culture media were purchased from Sigma Chemical Company (St. Louis, MO, USA) unless stated otherwise.

Care and handling of ICR mice was conducted in accordance with the Animal Research Committee guidelines promulgated by the Ethics Committee of the Institute of Zoology, Chinese Academy of Sciences.

IR and hyperandrogenism mouse model

Female ICR mice (18–20 g) (age 30–34 days) were divided into three groups: control, insulin-treated (INS-treated) and insulin-HCG-treated (INS-HCG-treated). The treatment protocol was composed of two s.c.

injections of saline (control mice), insulin (to produce hyperinsulinemia and IR) or insulin plus hCG (to produce hyperandrogenism) each day for 22 days (Lima *et al.*, 2006). Insulin injections were 0.05 IU until Day 16 after which they were gradually increased, reaching a daily total of 0.8 IU by Day 22 (Poretsky *et al.*, 1992; Lima *et al.*, 2006). HCG injections were given at 0.075 IU twice a day throughout. To collect GV oocytes, control, INS-treated and INS-HCG-treated mice were primed with 5 IU pregnant mare serum gonadotrophin (PMSG) by an i.p. injection, and 12 or 48 h later, GV oocytes were obtained by manual rupturing of antral ovarian follicles in M2 medium. To collect ovulated oocytes, control and experimental mice were injected with 5 IU hCG (Ningbo, China) 48 h after priming with 5 IU PMSG (Ningbo, China). Oocytes were recovered from oviductal ampullae 14 h after hCG, and cumulus cells were removed by brief incubation in 1 mg/ml hyaluronidase. Prior to oocyte collection, mice were culled by cervical dislocation. Blood samples were taken via cardiac puncture.

Oocytes were arrested at the GV stage in M2 medium supplemented with 2.5 μ M milrinone to prevent meiotic resumption during all experiments using live GV oocytes.

IVF and embryo culture

Spermatozoa were collected by squeezing excised the cauda epididymides of ICR male mice into a 600- μ l drop of modified human fallopian tube fluid (Irvine Science, Irvine, CA, USA) supplemented with 10% serum protein substitute (SPS; SAGE ART-3010) under mineral oil. Spermatozoa were capacitated in the same medium under mineral oil at 37°C, 5% CO₂ in air for 1.5 h. Ovulated oocytes were maintained in human tubal fluid media. Capacitated sperm (1×10^6 /ml) were added to cumulus-free eggs (50 eggs in 200 μ l capacitated sperm) at 37°C, 5% CO₂ in air for 6 h after which oocytes were removed and examined for fertilization. Oocytes with two pronuclei were cultured in KSOM (K Simplex Optimization medium) at 37°C, 5% CO₂ in air and examined for blastocysts after 5 days of culture.

Determination of ROS products

To determine the quantity of ROS production, cumulus-denuded GV and MII oocytes were loaded with the oxidation-sensitive fluorescent probe [dichlorofluorescein (DCFH)] by incubation for 30 min at 37°C in M2 medium (Sigma, USA) supplemented with DCFH diacetate (DCFH-DA) (2 μ M) (Beyotime Institute of Biotechnology, China) (Victor *et al.*, 2009). Oocytes were washed three times in M2 medium supplemented with bovine serum albumin (BSA) and mounted on glass slides. Fluorescence was measured using fluorescence microscopy (Zeiss LSM510 META) with 450–490 nm (excitation) and 520 nm (emission) filters. Images were taken at 10 (eye lens) \times 20 (objective) \times 3 (scan zoom)-fold magnification in an optical cross section through the centre of the oocyte at its largest nuclear diameter. The photographs were analyzed using Image J 1.240 software (Research Services Branch, National Institute of Mental Health, Bethesda, MD, USA), measuring brightness for each oocyte.

The intracellular H₂O₂ level in oocytes was analyzed using a commercial H₂O₂ assay kit (Beyotime Institute of Biotechnology) in which H₂O₂ oxidizes ferrous ions (Fe²⁺) to ferric ions (Fe³⁺) that then form a purple-colored complex with an indicator dye xylenol orange (3,3-bis[N,N-di(carboxymethyl)-aminomethyl]-o-cresolsulfone-phthalein, disodium salt). We detect the level of H₂O₂ by examining the colored complex by a microplate reader (Qian *et al.*, 2009; Tripathi *et al.*, 2009). Firstly, 30–50 oocytes from each group of the GV or MII stage were mixed with 100 μ l of schizolysis solution supplied by the kit for lysis on ice for 1 h; then the supernatants were collected by centrifuging at 11 000 rpm for 10 min at 4°C for the following tests. All the operations

were carried out on ice. Finally, the test tubes containing 100 μ l of supernatants and 100 μ l of test solutions were placed at room temperature for 20 min. A clear supernatant was removed from each group and stored at -70°C until use. The optical density was determined using a microplate reader (Bio-TEK, USA) set at 560 nm. The samples were run in triplicate and all samples were run in one assay to avoid variation.

Measurement GSH content

The concentrations of total glutathione (T-GSH), oxidized disulfide (GSSG) and reduced GSH were evaluated spectrophotometrically with a commercial assay kit (Beyotime Institute of Biotechnology) based on an enzymatic method according to the manufacturer's instructions. A total of 30–50 oocytes from each group of the GV or MII stage were mixed with 5 μ l of protein scavenger supplied by the kit and vortexed for 5 min; then the mixture was frozen at -70°C for 2 min and thawed at 37°C repeatedly for three times. The mixture was centrifuged at 10 000 rpm for 10 min at 4°C and put on ice for 5 min for the following tests. To examine the GSSG, we removed GSH with diethyl maleimide, 2-vinylpyridine. We examined the level of GSH and GSSG in only fresh oocytes according to the kit illustrations each time.

Quantification of ATP

The measurement of ATP content in oocytes was performed with a luminometer (Bioluminat Junior; Berthold, Wildbad, Germany) by using a commercial assay kit based on the luciferin–luciferase reaction (Beyotime Institute of Biotechnology), following the procedure described by [Combelles and Albertini, \(2003\)](#) and [Chen et al. \(2009\)](#) and the manufacturer's recommendations. A total of 30–50 oocytes from each group of GV or MII stage were mixed with 100 μ l of schizolysis solution supplied by the kit and vortexed for 1 min on ice for lysis, then the mixture was collected by centrifuging at 12 000 rpm for 10 min at 4°C and stored at -70°C until use. A 10-point standard curve (0, 0.01, 0.1, 0.5, 0.75, 1.0, 1.5, 2.0, 2.5 and 5.0 pmol of ATP) and three negative controls were included in each assay. Standard curves were generated and the ATP content was calculated by using the formula derived from the linear regression of the standard curve.

Determination of mitochondrial DNA copy number by quantitative real-time PCR

Mitochondrial DNA (mtDNA) quantitative real-time PCR procedures have been described previously ([Cao et al., 2007](#)). The mouse mtDNA-specific primers: B6 forward, AACCTGGCACTGAGTCACCA, and B6 reverse, GGGTCTGAGTGTATATATCATGAAGAGAAT ([Shitara et al., 2000](#); [Cao et al., 2007](#); [Wang et al., 2009](#)) were used to prepare the external standard for absolute quantification of mtDNA. PCR products were ligated into the T-vector. Seven 10-fold serial dilutions of purified plasmid standard DNA were made to produce a standard curve. Briefly, one oocyte was loaded in a PCR tube with 5 μ l of lysis buffer and incubated at 55°C for 2 h. Proteinase K was heat inactivated at 95°C for 10 min, and then the samples were used directly for PCR analysis. Quantitative real-time PCR was performed using the ABI system and above-mentioned mouse mtDNA-specific primers. The cycling conditions included an initial phase of 10 min at 95°C and 40 cycles of 15 s at 95°C and 1 min at 60°C . The melting temperature was 76.5°C . Linear regression analysis of all standard curves for samples showed a correlation coefficient higher than 0.97. All measurements were performed in triplicates.

Immunofluorescence

For mitochondrial staining or inner mitochondrial membrane potential staining, live denuded oocytes were cultured in M2 medium containing

200 nM MitoTracker Red (Molecular Probes, Eugene, OR, USA) or 2 μ M JC-1 fluorochrome (Beyotime Institute of Biotechnology) for 30 min at 37°C , 5% CO_2 in air ([Gualtieri et al., 2009](#)). After washes, oocytes were still incubated in M2 medium and analyzed by fluorescence microscopy at 37°C , 5% CO_2 in air (Zeiss LSM510 META). An image was taken at $10 \times 20 \times 2$ -fold magnification in an optical cross section through the centre of the oocyte at its largest nuclear diameter.

For spindle and chromosome analysis, oocytes were fixed with 4% paraformaldehyde for 30 min and then permeabilized with 0.5% Triton X-100 for 20 min. After blocking in 1% BSA-supplemented phosphate-buffered saline (PBS) for 1 h, samples were incubated for 2 h at room temperature with fluorescein isothiocyanate-conjugated α -tubulin antibody (1:200) to visualize microtubules in the spindle. Chromosomes were evaluated by co-staining with 4 μ M To-Pro-3-iodide (Molecular Probes) for 10 min. Samples were examined under a laser scanning confocal microscope (Zeiss LSM510 META). The filter used was LP 505, and the lasers for observing the chromosomes and the spindle were ultraviolet and FITC, respectively. An image was taken at $10 \times 40 \times 2$ -fold magnification in an optical cross section through the centre of the oocyte at its largest nuclear diameter.

Annexin-V staining of oocytes

Staining was performed with an Annexin-V staining kit according to the manufacturer's instructions (Beyotime Institute of Biotechnology). Briefly, live oocytes were washed twice in PBS and stained for 10 min in the dark with 195 μ l of binding buffer, which contained 5 μ l of Annexin-V-FITC. Fluorescence was measured using fluorescence microscopy (Zeiss LSM510 META) with 450–490 nm (excitation) and 520 nm (emission) filters.

Evaluation of cortical granule distribution by confocal laser scanning microscopy

Denuded oocytes were fixed with 4% (w/v) paraformaldehyde for 30 min at room temperature. After a 5-min treatment in PBS containing 0.1% Triton X-100, oocytes were washed two times in PBS. To label cortical granules (CGs), oocytes were cultured in FITC-labeled peanut agglutinin (100 mg/ml) M2 medium for 30 min in a dark box. The nuclear status of the oocytes was evaluated by staining with 10 mg/ml propidium iodide in PBS for 10 min. Finally, observation was performed using a laser scanning confocal fluorescent microscope (Zeiss LSM510 META) with 488 nm (excitation) and 543 nm (emission) filters. An image was taken at $10 \times 20 \times 2$ -fold magnification in an optical cross section. Scans were taken through the equatorial plane of the oocyte. Each treatment was repeated at least three times.

Radioimmunoassay

Testosterone, estradiol (E_2), LH and insulin were measured in all samples by radioimmunoassay (RIA), after hexane:ethyl acetate (3:2) extraction and celite column partition chromatography, as described previously ([Butler, et al., 2004](#)). The RIA for each analyte used an iodinated radioligand in conjunction with a highly specific antiserum. After a 14–16 h incubation period, a second antibody was used to separate the antibody-bound from the unbound steroid. The intra-assay and inter-assay coefficients of variation ranged from 5 to 9% and 11 to 14%, respectively, at low, medium and high levels of the five different steroid hormones in quality control ([Lima et al., 2006](#)).

Statistical analysis

Image processing was performed using an laser scanning microscopes Image Browser. Data (mean \pm SEM) were from at least three replicates

per experiment and analyzed by analysis of variance using SPSS software (SPSS Inc., Chicago, IL, USA) followed by the Fisher's least significant difference test. The number of oocytes observed was denoted in parentheses as (*n*). Difference at $P < 0.05$ or $P < 0.01$ were considered to be statistically significant and different superscripts indicate the statistical difference.

Results

Establishment of the IR and hyperandrogenism mouse model

To explore the effect of maternal IR and hyperandrogenism on female fertility, we established an insulin-resistant and hyperandrogenism mouse model through exogenous insulin and HCG injection (Lima *et al.*, 2006). Table I shows the effects of various treatments on the mouse weight, mean serum levels of insulin, glucose, LH, testosterone and E_2 . The weight, serum insulin, glucose and homeostatic model assessment (HOMA)-IR of INS-treated ($n = 15$) and INS-HCG-treated ($n = 15$) mice were higher compared with those in the control ($n = 12$) ($P < 0.05$). Although the maternal serum glucose level in the INS-treated and INS-HCG-treated groups was higher than that in the control group, the concentration of glucose was within the normal range. The serum testosterone level was significantly elevated in INS-HCG-treated mice compared with that of the INS-treated or the control group. In contrast, the serum E_2 concentration was

similar in all groups. These results show that the IR and hyperandrogenism models were successfully established.

Maternal IR decreases the ovarian response during controlled ovarian stimulus, affecting MII oocyte quality and early embryo development

To investigate the effect of IR on ovulation during controlled ovarian stimulus (COH), we examined the incidence of ovulation after injection of PMSG and HCG. As shown in Table II, the ovulation rate and the recovered oocyte number per mouse were significantly reduced during COH in INS-treated and INS-HCG-treated mice compared with the controls. Morphological abnormalities of MII oocytes were examined by stereomicroscopy. We found that 14 and 16.1% of oocytes from INS-treated ($n = 257$) and INS-HCG-treated ($n = 192$) mice showed abnormal morphological characteristics (Fig. 1A, black arrowheads), including (a) enlarged perivitelline space, (b) fragmented cytoplasm and (c) degraded polar bodies, which were significantly higher than those in the controls (7.1%, $n = 301$) (Fig. 1B). Subsequently, MII oocytes with normal appearance were chosen for further investigation.

The chosen MII oocytes were fertilized *in vitro*. Compared with the control (Fig. 1C), the fertilization ability of oocytes, cleavage rates and blastocyst rates in INS-treated and INS-HCG-treated mice significantly decreased (Table II, Fig. 1D) ($P < 0.05$). Moreover, insulin-resistant

Table I The effects of hyperinsulinemia on maternal weights, metabolic parameters and serum hormone levels.

	Control	INS	INS + HCG
N	12	15	15
Body weight (g)	29.9 ± 2.1	32.3 ± 2.1*	32.1 ± 1.8*
Serum glucose (mmol/l)	6.1 ± 0.5	8.0 ± 0.8*	7.7 ± 0.9*
Serum insulin (mU/l)	12.6 ± 2.2	27.4 ± 2.6*	27.9 ± 3.9*
HOMA (glucose × insulin/22.5)	3.5 ± 0.8	9.8 ± 1.8*	9.5 ± 1.6*
LH (mIU/ml)	0.085 ± 0.01	0.075 ± 0.01	0.1 ± 0.03***
E_2 (pg/ml)	82.6 ± 6.6	82.1 ± 7.4	80.9 ± 10.1
Serum-free testosterone (ng/dl)	53.2 ± 3.4	54.7 ± 5.2	81.8 ± 8.6***

* $P < 0.05$ versus control; ** $P < 0.05$ versus insulin-induced mice; values are mean ± SEM.

Table II The effects of maternal hyperinsulinemia on oocyte maturation and early embryo development.

Parameter	Control	INS	INS + HCG
Mice with retrieved oocytes/ <i>n</i> (%)	20/21 (95)	26/59 (44)*	23/58 (40)*
Number of oocytes recovered/mouse Mean ± SEM (<i>n</i>)	14 ± 2.3 (20)	8.5 ± 3.4 (26)*	7 ± 2.8 (23)*
Fertilization rates fertilized/total (%)	208/275 (76)	144/221 (65)*	100/161 (62)*
Cleaved embryos			
Cleaved/fertilized (%)	134/208 (64)	75/144 (52)*	51/100 (51)*
Blastocysts/cleaved embryos (%)	65/134 (48)	22/75 (29)*	16/51 (31)*

* $P < 0.05$ versus control; values are mean ± SEM.

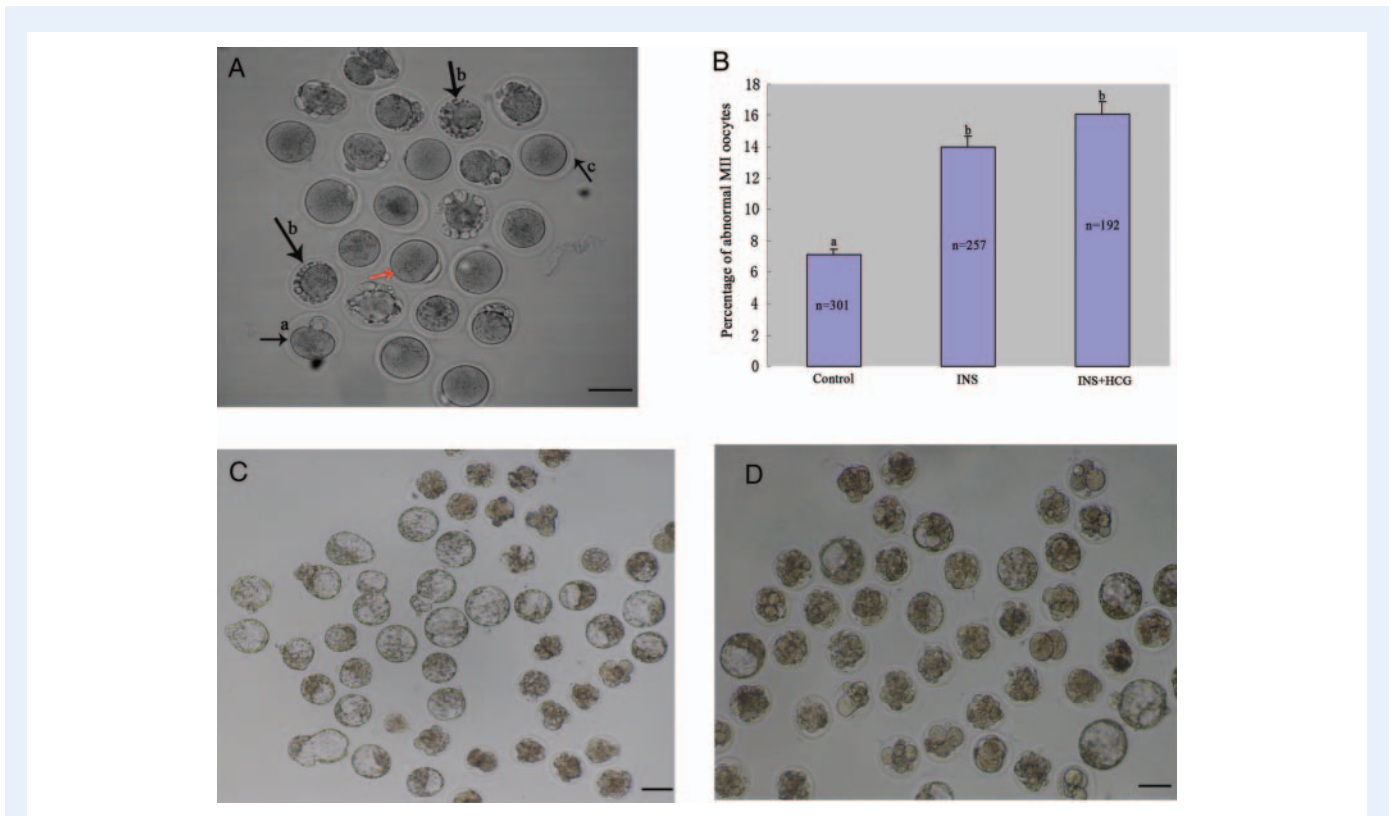


Figure 1 Morphological evaluation of ovulated oocytes and development of embryos *in vitro* from insulin-resistant mice. **(A)** Images of MII oocytes recovered from hyperinsulinemic mice. Red arrowheads denote oocytes with normal appearance, (a) enlarged perivitelline space; (b) fragmented cytoplasm and (c) degraded polar bodies are indicated by black arrowheads; **(B)** Percentage of abnormal MII oocytes from control, INS-treated and INS-HCG-treated groups; *n* shows the number of oocytes derived from at least three independent experiments. Different letters indicate statistically significant differences ($P < 0.05$); **(C)** Development of control embryos after 5 days of culture; **(D)** Development of embryos derived from oocytes from INS-treated mice after 5 days of culture. (Embryos in the INS + HCG-treated groups showed similar features as the INS-treated mice.) Bar = 10 μ m.

mice featured embryos with increased fragmentation (Fig. 1D). Taken together, maternal IR significantly affects oocyte maturation and early embryonic development.

The ROS level abnormally increases in the GV and MII oocytes of insulin-resistant mice

To evaluate OS in oocytes, we measured the level of intracellular ROS. The DCFH-DA fluorescence intensity was significantly higher in the GV oocytes of the INS-treated and INS-HCG-treated groups than that in the control, indicating an augmented production of ROS [Fig. 2A and B(a–d); $P < 0.01$]. The DCFH-DA fluorescence intensity of MII oocytes from the INS-treated to INS-HCG-treated groups notably increased compared with the control [Fig. 2C and Da and b; $P < 0.01$]. Moreover, ROS distribution in MII oocytes from the INS-treated to INS-HCG-treated groups was aggregated into clumps in the cytoplasm (arrow) (Fig. 2Dd–f). We also examined the H_2O_2 levels in all groups. With the meiotic resumption, the H_2O_2 level from the GV to MII stages showed a significant increase (GV, 54.2 ± 2.4 ng/oocyte versus MII, 67.5 ± 1.3 ng/oocyte; $P < 0.05$). Moreover, the H_2O_2 level in GV oocytes from the INS-treated (65.6 ± 2.0 ng/oocyte) and INS-HCG-treated mice (65.1 ± 1.7 ng/oocyte) increased when compared with the control (Fig. 2E). H_2O_2 levels further increased

in the MII oocytes of INS-treated and INS-HCG-treated mice compared with the control (84.8 ± 2.5 and 86.2 ± 2.1 versus 67.5 ± 1.3 ng/oocyte, control; $P < 0.01$) (Fig. 2F).

Antioxidant functions are reduced in oocytes from insulin-resistant mice

We determined whether or not the antioxidant capacity of oocytes was impaired. Figure 3A shows a significantly lower reduced GSH level in GV oocytes of INS-treated (0.92 ± 0.03 pmol/oocyte) and INS-HCG-treated (1.04 ± 0.045 pmol/oocyte) mice when compared with the controls (1.98 ± 0.03 pmol/oocyte). It was followed by decreased GSH/GSSG in the GV oocytes of the INS-treated and INS-HCG-treated groups when compared with the controls (Fig. 3B). Furthermore, reduced GSH was significantly lower in the MII oocytes of the INS-treated (2.0 ± 0.04 pmol/oocyte) and INS-HCG-treated groups (1.94 ± 0.06 pmol/oocyte) compared with the control (3.03 ± 0.07 pmol/oocyte) (Fig. 3C). Moreover, MII oocytes from the INS-treated to INS-HCG-treated groups showed a significantly lower ratio of GSH/GSSG compared with the control ($P < 0.05$) (Fig. 3D). Together, these results suggest that the antioxidant functions are disrupted in insulin-resistant mice.

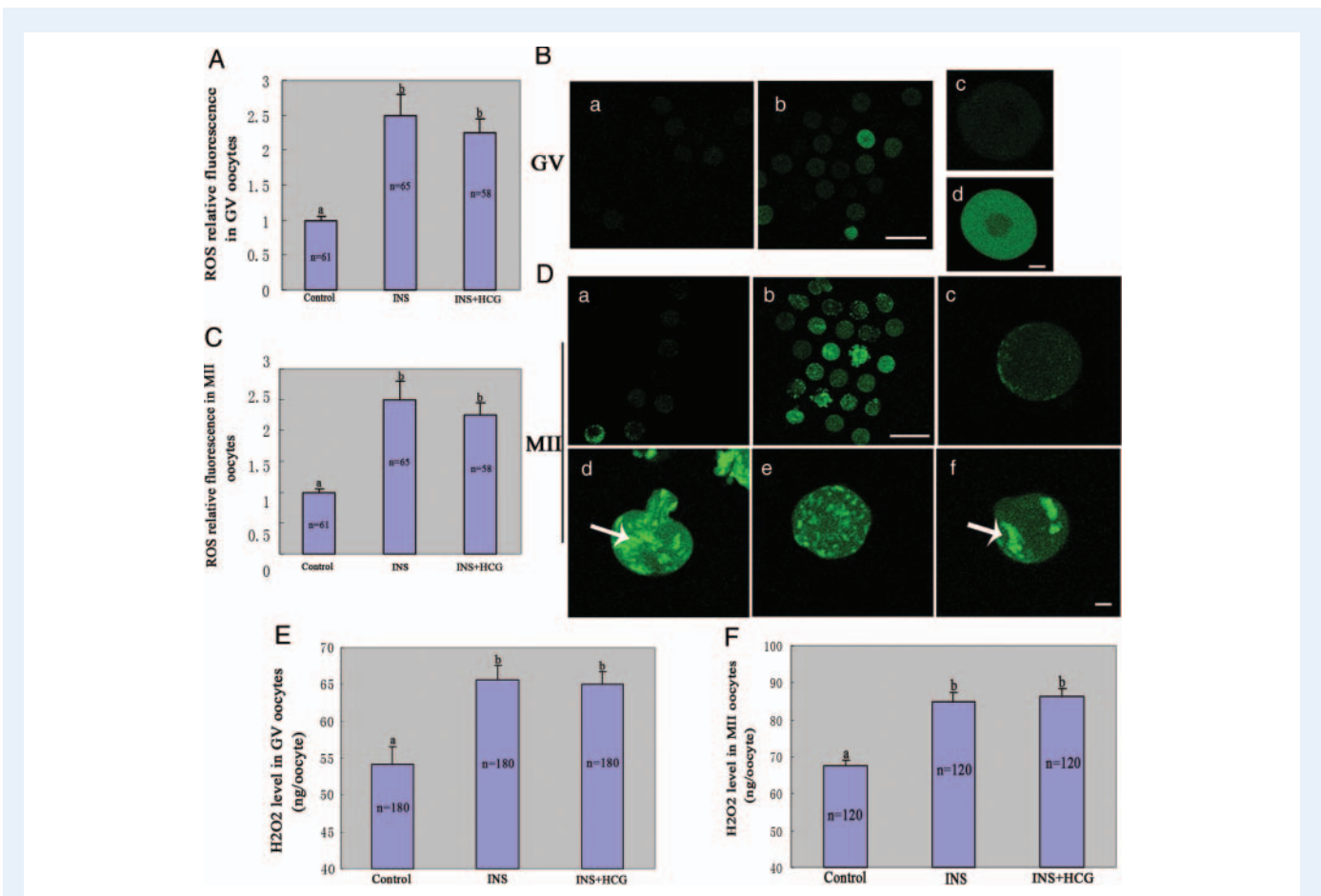


Figure 2 Effects of IR on ROS in GV and MII oocytes. **(A)** Effect of hyperinsulinemia on ROS production measured by the DCFH fluorescence in GV oocytes. **(B)** Changes in ROS production measured as the DCFH fluorescence; seen in representative images of GV oocytes: (Ba) control group, (Bb) hyperinsulinemic group, (Bc) a magnified view of one oocyte from Ba, (Bd) a magnified view of one oocyte from Bb. **(C)** Effect of hyperinsulinemia on ROS production measured by the DCFH fluorescence in MII oocytes; **(D)** Changes in ROS production measured as the DCFH fluorescence; seen in representative images of MII oocytes; (Da) control group, (Db) hyperinsulinemic group, (Dc) a magnified view of one oocyte from 'Da', [D(d–f)] magnified views of individual oocytes from 'Db', note that sources of ROS were aggregated into clumps in the cytoplasm (arrows in Dd and Df); **(E)** and **(F)** Intracellular levels of H₂O₂ in GV and MII oocytes from the control and hyperinsulinemic groups. In A, C, E and F, data are mean \pm SEM of three replicates, *n* shows the number of oocytes and different letters indicate statistically significant differences ($P < 0.01$).

MII oocytes from insulin-resistant mice show decreased mtDNA

Quantitative real-time PCR was performed on single fully grown GV and MII oocytes. mtDNA copy numbers in GV oocytes in the INS-treated and INS-HCG-treated groups showed no difference from those of the controls ($362\,000 \pm 27\,900$ and $365\,000 \pm 23\,500$ versus $364\,000 \pm 25\,800$, control; $P > 0.05$). However, the average mtDNA copy numbers in MII oocytes from INS-treated to INS-HCG-treated mice were significantly decreased compared with the control ($346\,000 \pm 13\,400$ and $354\,000 \pm 13\,000$ versus $430\,000 \pm 15\,200$, control; $P > 0.05$) (Fig. 4).

Maternal IR and hyperinsulinemia compromise mitochondrial function in GV and MII oocytes

Based on the mtDNA alterations in MII oocytes, we explored whether maternal hyperinsulinemia and IR influenced mitochondrial functions

of GV and MII oocytes. Interestingly, we found that the average ATP level in GV oocytes from the INS-treated (0.82 ± 0.02 pmol) to INS-HCG-treated mice (0.83 ± 0.01 pmol) was significantly higher than that in the control (0.65 ± 0.01 pmol). However, no difference between the INS-treated and INS-HCG-treated groups was observed (Fig. 5A). In contrast, MII oocytes in INS-treated and INS-HCG-treated groups exhibited significantly lower ATP content than the control group (Fig. 5B). The ATP levels in MII oocytes from the INS-treated to INS-HCG-treated groups were, respectively, 0.67 ± 0.02 and 0.69 ± 0.01 pmol, while the value was 0.91 ± 0.02 pmol in the control group ($P < 0.01$).

Maternal IR and hyperinsulinemia disrupt mitochondrial redistribution in GV and MII oocytes

Oocyte maturation is accompanied by distribution changes of active mitochondria. The present data show that the majority of the

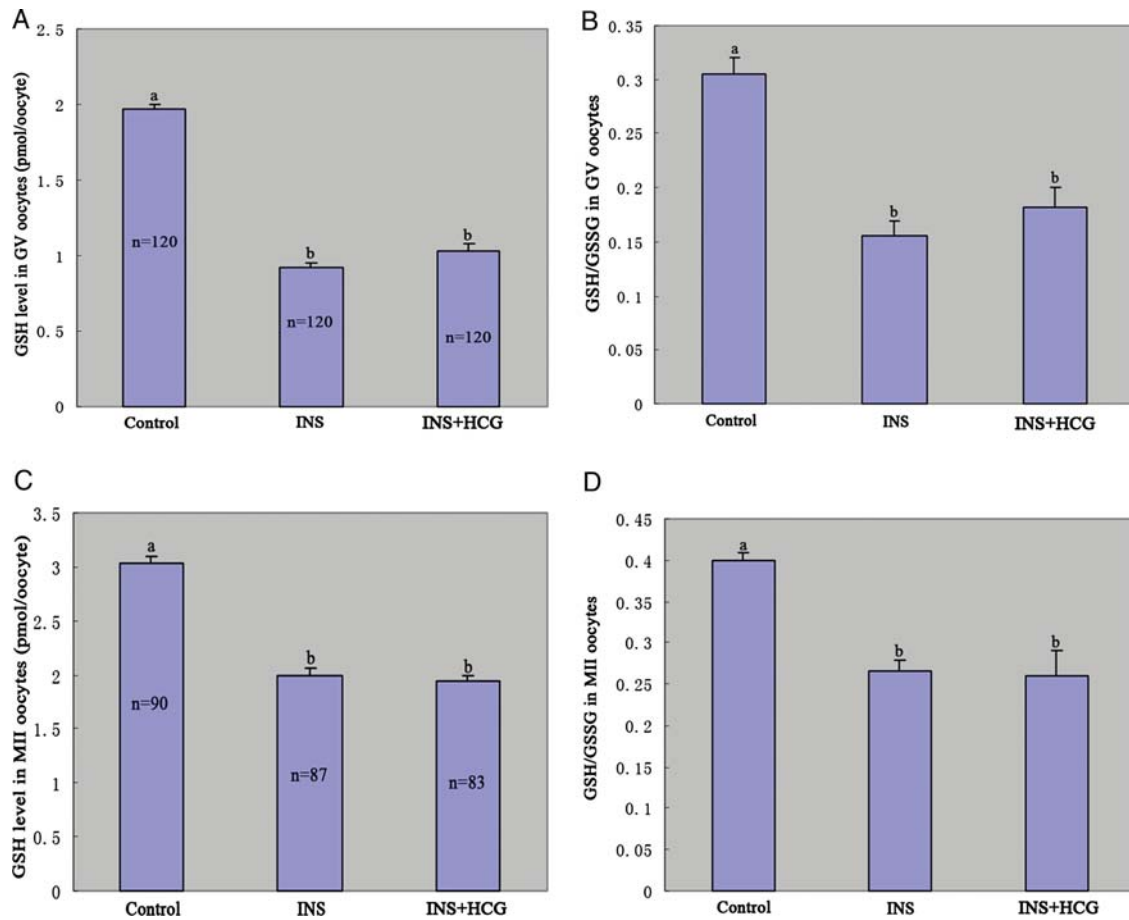


Figure 3 Effects of hyperinsulinemia on GSH levels in GV and MII oocytes. **(A)** The GSH concentration in GV oocytes; **(B)** The GSH:GSSG ratio in GV oocytes. **(C)** The GSH concentration in MII oocytes. **(D)** The GSH:GSSG ratio in MII oocytes. Data are mean \pm SEM from three replicates, n shows the number of oocytes and different letters indicate statistically significant differences ($P < 0.05$).

control GV oocytes displayed a homogeneous mitochondrial distribution pattern (68%), while 25.0% showed a perinuclear mitochondrial distribution pattern (Fig. 6Aa and b and B) 12 h after PMSG treatment. However, clustered mitochondria were observed throughout the cytoplasm in INS-treated (44%) and INS-HCG-treated (47%) GV oocytes (Fig. 6Ac and b) resulting in mitochondria occupying most of the oocyte volume. At 48 h of PMSG treatment, 67% of the GV oocytes showed a perinuclear mitochondrial distribution in the control mouse, whereas clustered mitochondrial distribution was found in hyperinsulinemic GV oocytes [INS-treated group (47%); INS-HCG-treated group (41.7%)] (Fig. 6C). With the completion of meiotic maturation, the polarized mitochondrial distribution in MII oocytes was reduced in the INS-treated and INS-HCG-treated groups when compared with the control group (Fig. 6Da) (30, 31 versus 61% control, $P < 0.05$), whereas the proportion of the homogeneous distribution (Fig. 6Db) increased in the INS-treated and INS-HCG-treated groups (43, 38 versus 26%, control, $P < 0.05$) (Fig. 6E). Interestingly, the distribution of heterogeneous mitochondria in large clumps (arrow) Fig. 6Cc also increased in the INS-treated and INS-HCG-treated groups compared with the control group (27, 31 versus 13%, $P < 0.05$) (Fig. 6Dc and E).

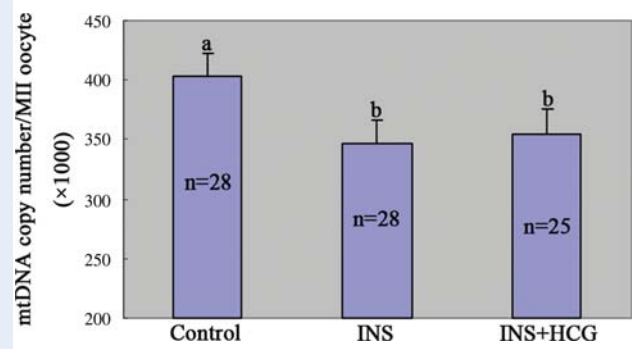


Figure 4 The effect of hyperinsulinemia on the mtDNA copy number in single MII oocytes determined by quantitative real-time PCR. Data are mean \pm SEM from at least three independent experiments, n shows the number of oocytes and different letters indicate statistically significant differences ($P < 0.05$).

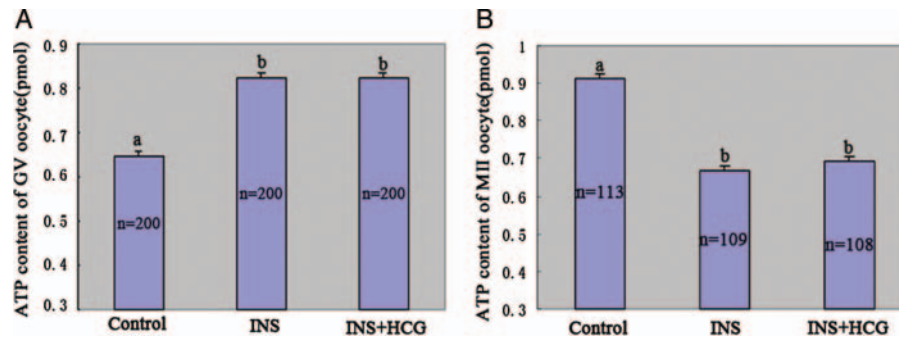


Figure 5 The effect of hyperinsulinemia on ATP levels. **(A)** GV oocytes and **(B)** MII oocytes. Data are mean \pm SEM, *n* shows number of oocytes and different letters indicate statistically significant differences ($P < 0.01$).

Maternal IR and hyperinsulinemia affect the inner mitochondrial membrane potential in GV and MII oocytes

At an inner mitochondrial membrane potential ($\Delta\Psi_m$) < 100 mV, JC-1 remain a monomer and emits green fluorescence in the FITC channel (low polarized mitochondria), whereas at $\Delta\Psi_m > 140$ mV, it forms J-aggregates and emits red fluorescence in the rhodamine isothiocyanate channel (high polarized mitochondria) (Reers *et al.*, 1995). We investigated the high polarization of mitochondria in GV and MII oocytes by examining the relative level of red to green fluorescence emission. Relative inner membrane potential in GV oocytes 48 h after PMSG from the INS-treated ($n = 78$) and INS-HCG-treated ($n = 72$) mice sharply increased, compared with the control ($n = 70$) (2.09, 2.19 versus 1.21, $P < 0.01$), (Fig. 7A and B), indicating an increased $\Delta\Psi_m$. In contrast, relative $\Delta\Psi_m$ in MII oocytes from INS-treated ($n = 82$) to INS-HCG-treated ($n = 76$) mice sharply decreased, compared with the control ($n = 71$) (0.76, 0.81 versus 1.66, $P < 0.01$) (Fig. 7C and E), indicating a reduced or collapsed $\Delta\Psi_m$. In particular, the mitochondria in 93% MII oocytes of the control group showed high polarity in the pericortical cytoplasm. However, 34 and 32% MII oocytes of the INS-treated and INS-HCG-treated groups were characterized by patchy (Fig. 7Ca) and low-polarized (Fig. 7Cb) mitochondria in the pericortical cytoplasm, with clustered green fluorescence in the deeper cytoplasm (Fig. 7Cc and D). Taken together, these results suggest that maternal IR leads to abnormal $\Delta\Psi_m$ during oocyte maturation.

Maternal IR contributes to early apoptosis of GV oocytes

Annexin-V, a phospholipid-binding protein, detects the translocation of the phospholipid phosphatidylserine (PS) from the inner to the outer cytoplasmic membrane, which is known to occur during the early stages of apoptosis (Martin *et al.*, 1995). Only the morphologically normal oocytes were analyzed. As shown in Fig. 8Aa and b (arrows), PS cannot translocate into the inner membrane, and oocytes with green fluorescence signals only at the zona pellucida were viable and non-apoptotic. GV oocytes with early apoptosis are characterized by a clear green signal in the oocyte membrane (Fig. 8Ac, arrow). As shown in Fig. 8B, the early apoptosis rate of GV

oocytes 48 h after PMSG from the INS-treated (22.8%, $n = 101$) to INS-HCG-treated mice (20.2%, $n = 94$) was significantly higher than that from the control group (4.3%, $n = 93$). However, there was no difference between the INS-treated and INS-HCG-treated groups. The results suggest that IR may promote early events associated with apoptosis of GV oocytes.

Maternal IR affects the distribution of CGs in MII oocytes

Systematic comparative studies of the CG redistribution can be a helpful marker to identify oocyte cytoplasmic maturation; a large second CG-free domain (CGFD) is formed in the MII oocytes. We found that *in vivo* MII oocytes from the hyperinsulinemic mouse model showed higher partial premature CG exocytosis (INS-treated, 23.9%; INS-HCG-treated, 26.7%) than the control oocytes (8.8%) ($P < 0.01$) (Fig. 9A and B).

Maternal IR is associated with abnormal spindles and misaligned chromosomes

Next, we examined the spindle and chromosomes of MII oocytes from the INS-treated to INS-HCG-treated mice by confocal scanning microscopy. As shown in Fig. 10A, most of the MII oocytes in the control group exhibited barrel-shaped spindles and well-aligned chromosomes. However, 16.9 and 18.1% defective spindles were observed in the INS-treated and INS-HCG-treated mice, respectively, compared with 6.7% in the control (Fig. 10B). The defective spindles include disintegrated spindle poles, additional asters and abnormal spindle shapes (Fig. 10Aa and b). Oocytes in the INS-treated (13.6%, $n = 78$) and INS-HCG-treated (15.5%, $n = 93$) mice displayed severe defects in chromosome alignment, showing lagging chromosomes and irregularly scattered chromosomes (Fig. 10Ac and d), which were considerably higher than in the control group (5.5%, $n = 87$) ($P < 0.01$) (Fig. 10B).

Discussion

This study revealed that IR leads to the imbalance between oxidants and antioxidants associated with OS in the oocyte's cytoplasm and impairs mitochondrial function in oocytes. We created IR and hyperandrogenized mouse models by treatment with insulin alone and by

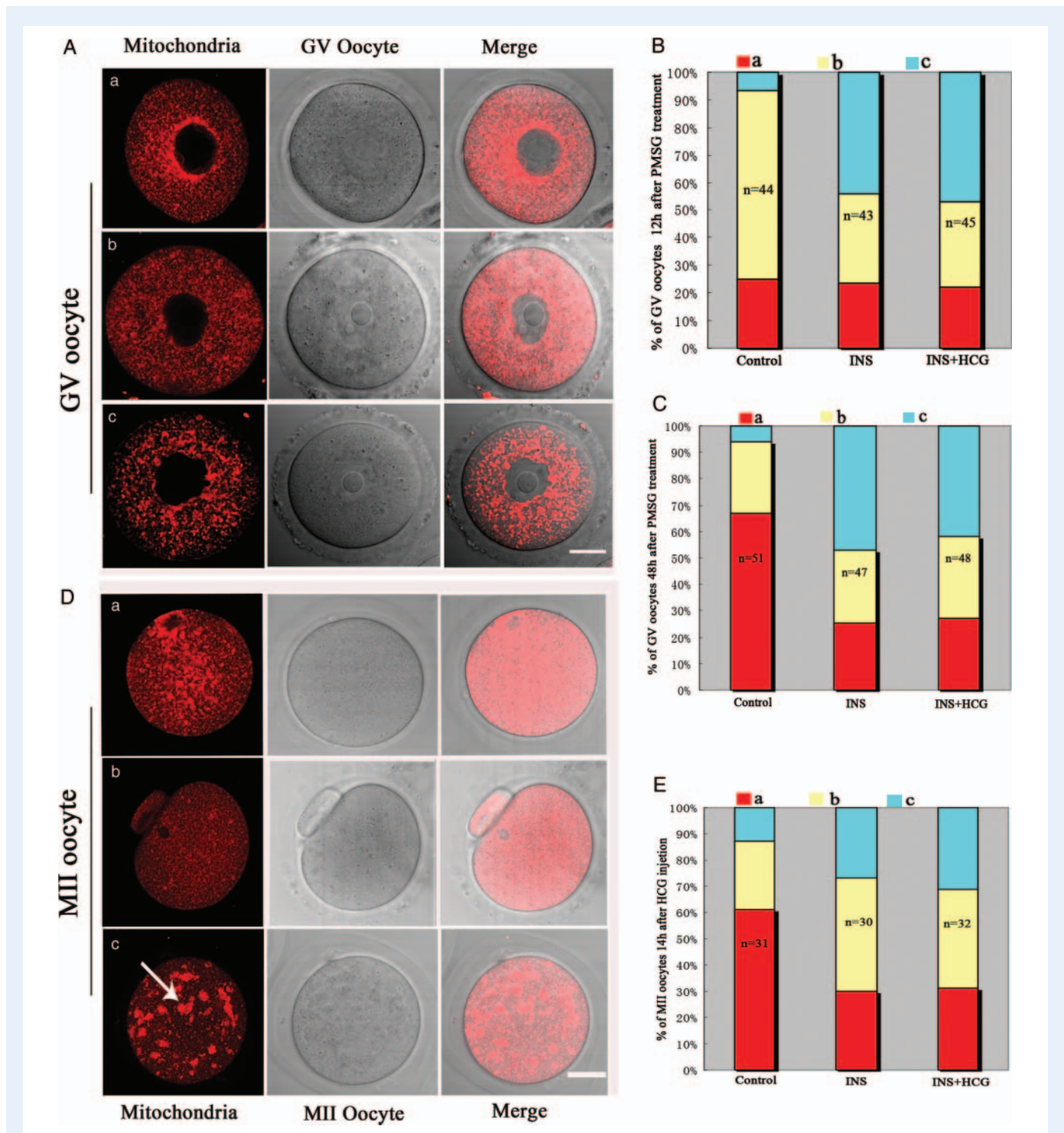


Figure 6 The effect of hyperinsulinemia on the mitochondrial redistribution in GV and MII oocytes. **(A)** Mitochondrial distribution patterns in GV oocytes detected by fluorescence microscopy using MitoTracker Red: (a) perinuclear distribution, (b) homogeneous distribution and (c) clustered distribution; **(B)** Proportion of GV oocytes recovered 12 h after PMSG to show each mitochondrial distribution pattern; *n* shows the number of oocytes; **(C)** Proportion of GV oocytes retrieved 48 h after PMSG treatment; **(D)** Mitochondrial distribution patterns seen in MII oocytes recovered 14 h after HCG to show each mitochondrial distribution pattern described in C, (a) polarized distribution, (b) homogeneous distribution and (c) large heterogeneous clump distribution; *n* shows the number of oocytes; **(E)** Proportion of MII oocytes recovered 14 h after HCG to show each mitochondrial distribution pattern described in D, *n* shows the number of oocytes. Bar = 10 μ m.

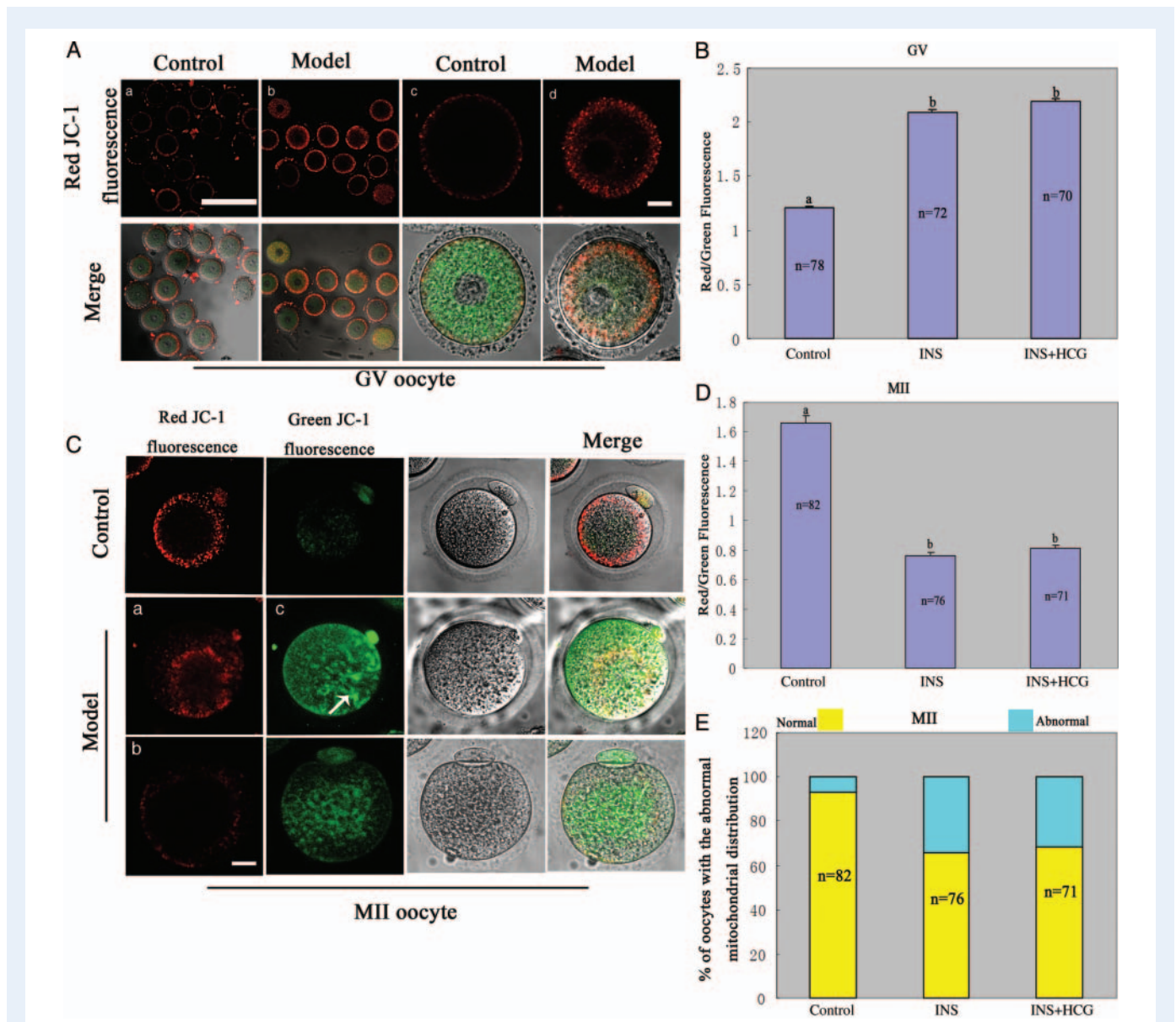


Figure 7 Effects of hyperinsulinemia on the inner mitochondrial membrane potential measured by JC-1 fluorescence in GV and MII oocytes. **(A)** and **(B)** The relative mitochondrial inner membrane potential ($\Delta\Psi_m$) in GV oocytes 48 h after PMSG. (Aa) JC-1 red fluorescence from the control; (Ab) JC-1 red fluorescence from the hyperinsulinemic group (model). (Ac) a magnified view of one oocyte from 'Aa', (Ad) a magnified view of one oocyte from 'Ab'. a,b (Bar = 20 μm); c,d (Bar = 10 μm). **(B)** Red/green fluorescence intensity in GV oocytes from the control and hyperinsulinemic group (model); **(C)**, **(D)** and **(E)** Relative $\Delta\Psi_m$ in MII oocytes from control and hyperinsulinemic groups. Red particulate fluorescence localized in the pericortical cytoplasm showed the high polarized mitochondria in most MII oocytes from the control group; green fluorescence localized in the deeper cytoplasm indicated the low polarized mitochondria. (Ca) Discontinued mitochondria; (Cb) low polarized mitochondria in the pericortical cytoplasm; (Cc) clustered green fluorescence (arrow) in the deeper cytoplasm was found in MII oocytes from hyperinsulinemic groups (Bar = 10 μm). **(D)** Red/Green fluorescence intensity in MII oocytes was examined in all groups. **(E)** Percentage of MII oocyte in each group that exhibited abnormal and normal polarized mitochondrial distribution. *n* shows the number of oocytes. Different letters denote statistically significant differences ($P < 0.05$).

treatment with insulin plus HCG, respectively (Lima *et al.*, 2006). Simultaneously, we used the mice fed with specific diets (data not presented), and found that the present results from insulin administration were basically the same as the results from the mice fed with specific diets. In addition, due to rapid spontaneous activation during *in vitro* handling, rat insulin-resistant models are not suitable for studying oocytes *in vitro* (Ross *et al.*, 2006, Yoo and Smith, 2007). Thus, we

chose the present insulin-resistant mouse model because of its high performance.

The results from the INS-treated and INS-HCG-treated groups were similar and thus, we propose that hyperinsulinemia, but not hyperandrogenism, may play a key role in impaired developmental potential of oocytes and embryos. Interestingly, GV oocytes from insulin-resistant mice showed higher metabolic activity. Conversely, MII

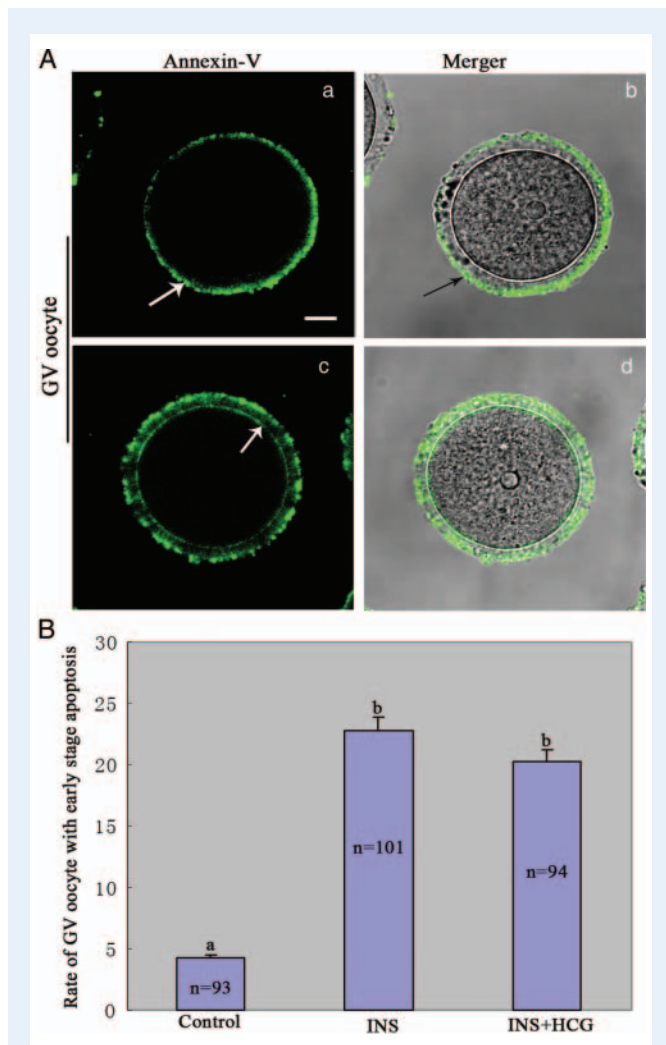


Figure 8 Hyperinsulinemia induced early-stage apoptosis of GV oocytes. **(A)** GV oocytes recovered 48 h after PMSG and stained with FITC-conjugated antibody to Annexin-V. (a, b) a viable oocyte; (c, d) an oocyte exhibiting early-stage apoptosis; (a, c) Annexin-V fluorescence; (b, d) merged fluorescence and confocal images. (Bar = 10 μ m) Note: viable oocytes only show fluorescence on the zona (arrow, a), whereas oocytes in early apoptosis also show fluorescence on the oocyte membrane (arrow, b). **(B)** The percentage of GV oocytes displaying early-stage apoptosis. Data are mean + SEM from at least three independent experiments and *n* shows the number of oocytes. Different letters denote statistically significant differences ($P < 0.01$).

oocytes from insulin-resistant mice showed lower mitochondrial metabolic activity. However, both GV and MII oocytes showed OS. Thus the effects of IR are complex and cell-stage specific.

Imbalance between ROS and antioxidant products leads to OS in oocytes of insulin-resistant mice

In a biological system, mitochondria and NADPH oxidase are the major sources of ROS production (Valko et al., 2007). ROS serves as a key signal molecule in the physiological processes, such as

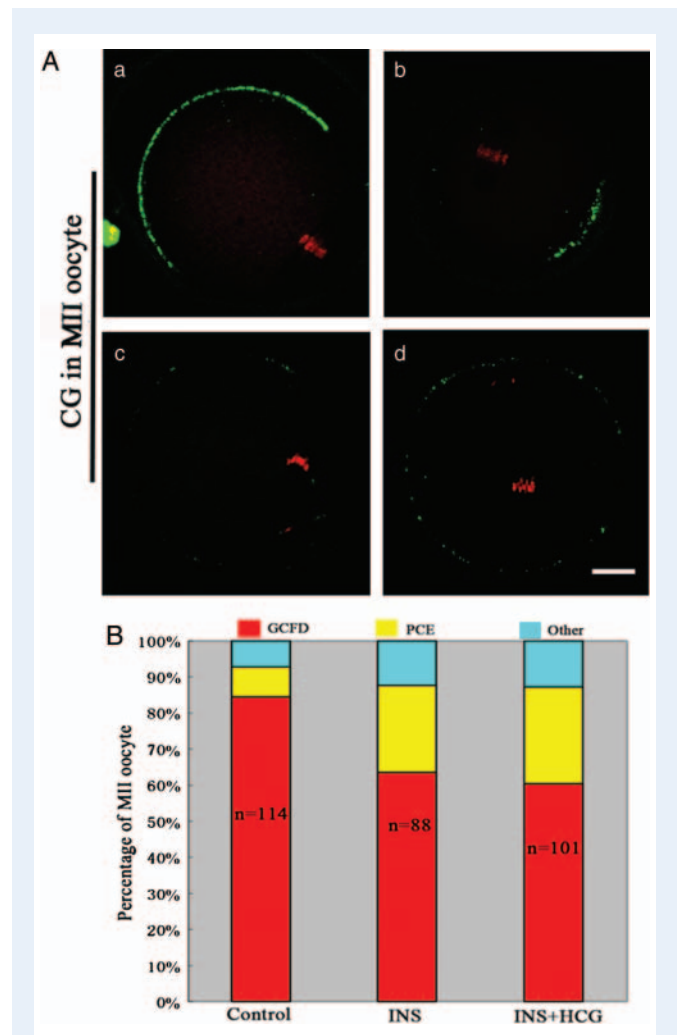


Figure 9 Hyperinsulinemia impairs the CG distribution in MII oocytes collected 14 h after HCG. **(A)** Confocal microscopic images (equatorial sections) of CGs (green) and chromatin (red) in MII oocytes. Aa is a representative image of a control MII oocyte with a CGFD, Ab–d show an MII oocyte from a hyperinsulinemic mouse that exhibits a premature partial CG exocytosis (PCE) (Bar = 10 μ m). **(B)** The percentage of MII oocytes with CGFD, PCE and other disorders in each group. The proportions of MII oocytes with PCE were higher in the hyperinsulinemic groups than in the control ($P < 0.01$).

meiotic resumption, but also plays a role in pathological processes such as cell apoptosis and senescence (Agarwal et al., 2005, Tripathi et al., 2009). Moreover, the insulin response is amplified by a pro-oxidative shift in the intracellular GSH redox state (Djurovic et al., 1997). In addition, high insulin can promote H_2O_2 production (Krieger-Brauer et al., 1997). Victor et al. (2009) reported the association between IR and an impaired mitochondrial oxidative metabolism, and proposed that OS in leukocytes was responsible for PCOS patients with IR. A markedly increased level of C-reactive protein was found in the follicular environment of obese women and this was often associated with increased ROS and OS, which may be associated with poor oocyte development (Robker et al., 2009). Thus, IR may contribute to excessive ROS in GV and MII oocytes. The pre-

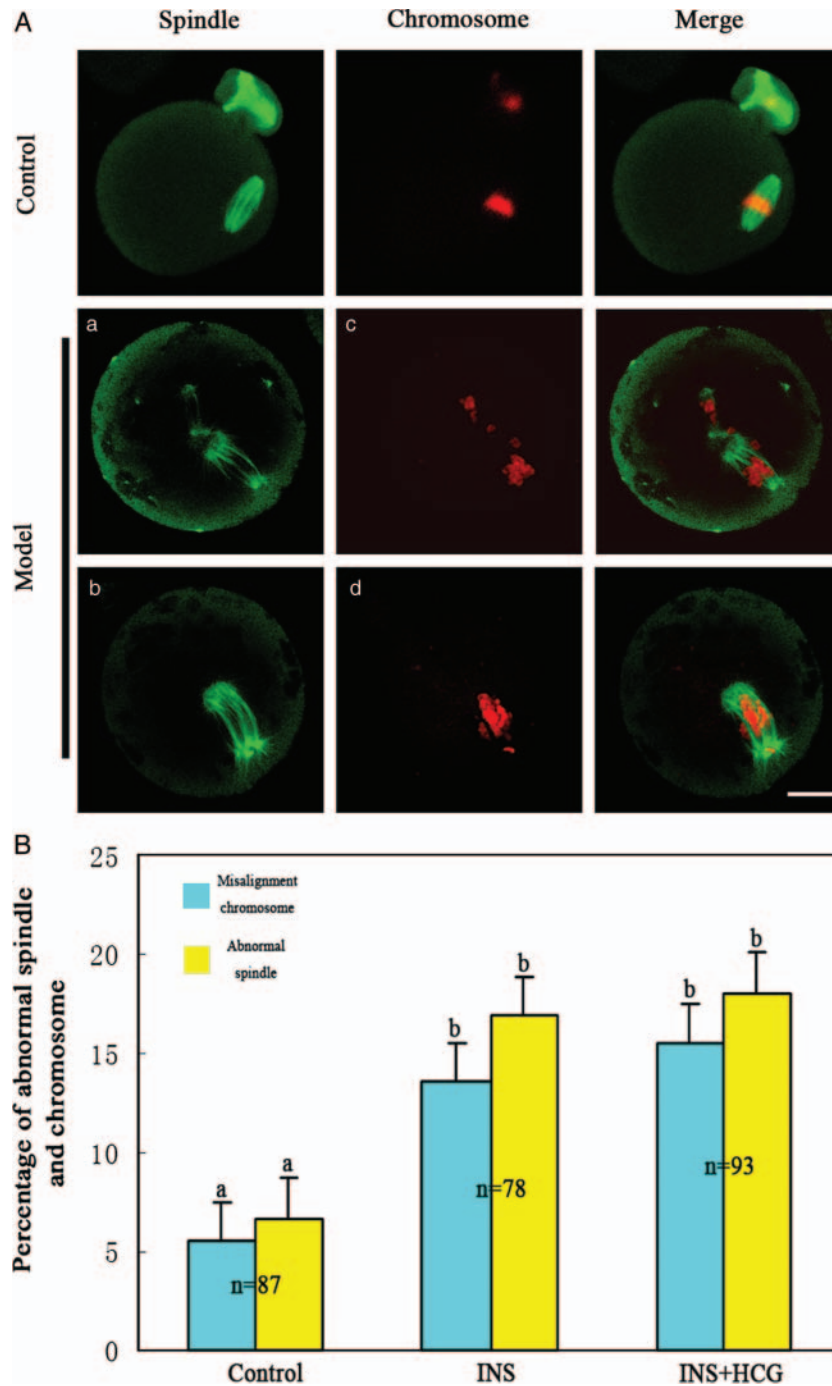


Figure 10 Hyperinsulinemia leads to defective spindles and misaligned chromosomes. **(A)** Representative images of the spindles and chromosomes in control and model groups. Normal spindle and aligned chromosomes are seen in the control group; misaligned chromosomes were detected in model groups. Figures Aa and b show the defective spindles, including disintegrated spindle poles, additional asters and abnormal spindle shapes; Figures Ac and d show lagging chromosomes and irregularly scattered chromosomes. α -Tubulin (green); DNA (red). (Bar = 10 μ m); **(B)** Percentage of oocytes with abnormal spindle and misaligned chromosomes in MII oocytes from control and hyperinsulinemic groups, data are mean \pm SEM of at least three independent experiments, *n* shows number of oocytes. Different letters denote statistically significant differences ($P < 0.01$).

ovulatory follicle has potent antioxidant defenses including the GSH (Jozwik *et al.*, 1999). The GSH serves as an efficient scavenger and plays a vital role in maintaining oocytes in a reduced environment, protecting them from OS. Overproduction of ROS, decreased GSH and

the reduced ratio of GSH/GSSG indicated the progression of OS in IR mice (Goud *et al.*, 2008). Moreover, mammalian oocytes and embryos are extremely sensitive to OS, and a slightly higher level of OS can disrupt oocyte maturation and embryo development, promoting

embryo fragmentation (Liu et al., 2000; Harvey et al., 2002; Van Blerkom, 2011). The results of the present study are consistent with the idea that OS induces the apoptosis of oocytes in insulin-resistant mice, characterized by lower recovered oocytes and increased embryo fragmentation (Liu et al., 2000).

Maternal IR disrupts mitochondrial function in oocytes

It has always been debated whether IR may be the primary event that impairs the mitochondrial function, although, very recently, it was demonstrated that IR may promote mitochondrial dysfunction (Sleigh et al., 2011). Our present results indicate that IR is associated with severely disrupted mitochondrial function in oocytes. Oocyte maturation includes nuclear and cytoplasmic maturation, and the mitochondrial status can be used to estimate cytoplasmic maturation in MII oocytes. Mitochondria are also among the most important organelles in the cytoplasm, and their distribution, $\Delta\Psi_m$ and the capacity of oxidative phosphorylation generating ATP as well as mtDNA copy number play important roles during oocyte maturation (Van Blerkom et al., 2003).

Reports indicate that sub-normal mtDNA levels could be directly associated with diminished oocyte competence and fertilization failure (Spikings et al., 2007; Mtango et al., 2008). In addition, preimplantation embryonic mtDNA composition is dependent on the number of oocyte mtDNA copies present at fertilization, because new mtDNA replication is only initiated post-implantation (Cummins, 2002). Although Wai et al. (2010) reported that the mtDNA number variability in mammalian oocytes did not seem to affect the egg's physiology, our results showed that a decreased mtDNA copy number in MII oocytes was associated with poor oocyte quality and reduced fertilization. At the MII stage, the loss of mtDNA associated with hyperinsulinemia may be due to degradation or autophagy. Moreover, mitochondria in an individual are maternally inherited and are the most abundant organelles in both oocytes and preimplantation embryos. It is proposed that the altered mtDNA copy number in MII oocytes may be implicated in a variety of inherited metabolic diseases in the offspring (Wallace, 2010). In addition, a significantly decreased mtDNA copy number and OS lead to ATP biosynthesis defects in MII oocytes that are associated with poor oocyte quality, low fertilization rates, and detrimental embryonic development in insulin-resistant mice (Thouas et al., 2004).

During oocyte maturation, the mitochondrial distribution is an important prerequisite for egg activation, fertilization and embryo development (Brevini et al., 2005). Decreased ATP supply and OS may lead to abnormal oocyte mitochondrial redistribution and large heterogeneous mitochondrial fragmentation, and thus insufficient energy provided to the nuclei and other organelles, which may be a cause for the retardation of MII oocyte developmental and arrest in insulin-resistant mice.

$\Delta\Psi_m$ may be involved in material transport and energy transition. Higher polarized mitochondrial clusters are localized within the pericortical region in maturing oocytes, which is linked to high ATP supply. Blerkom demonstrated that $\Delta\Psi_m$ was related to intercellular contact and communication (Van Blerkom et al., 2006). Therefore, reduced mitochondrial ATP content and mtDNA may account for low polarity in MII oocytes in insulin-resistant mice.

Furthermore, mtDNA lack histones, making them prone to oxidative injury (Madsen-Bouterse et al., 2010). Moreover, mitochondria are the major ROS generator, which renders them the first cell organelles to be affected (Carriere et al., 2006). Maternal hyperinsulinemia leads to OS in oocytes. OS appears to play a major role in mitochondrial dysfunction (Evans et al., 2002), whereas impaired mitochondria, in turn, produce more ROS, resulting in a vicious cycle.

Taken together, maternal IR contributes to OS and further disrupts mitochondrial function, leading to poor oocyte quality.

Maternal IR disrupts the development of premature oocytes

IR exerts different effects on GV and MII oocytes. In hyperinsulinemic mice, aggregated mitochondrial clusters and higher $\Delta\Psi_m$ in GV oocytes denote high metabolism. Interestingly, GV oocytes did not show increased mtDNA copy numbers in insulin-resistant mice. Thus, the results indicate that the oxidant metabolism in GV oocytes increases in hyperinsulinemic mice. Moreover, the perinuclear mitochondrial distribution showed no notable increase 48h after PMSG injection, which may confirm GV oocyte maturation arrest. Maternal diabetes delays meiotic maturation of GV oocytes by adversely affecting cAMP-activated protein kinase activity and cellular metabolism in murine oocytes (Ratchford et al., 2007). Insulin can increase mitochondrial transcript levels and ATP production in healthy people, but not in people with type 2 diabetes (Stump et al., 2003). Nagano reported that unusually high levels of ATP in the ooplasm at the GV stage may indicate a disruption of oocyte functions for ATP consumption, leading to low maturation and a subsequent decreased developmental ability (Nagano et al., 2006). IR is associated with decreased mitochondrial numbers and lower ATP synthesis in human muscle (Petersen et al., 2004). The reason why IR causes increased metabolism in GV oocytes requires further investigation.

Maternal IR compromises organelles in oocyte cytoplasm

Changes in the redox state and the mitochondrial activity contribute to defects in spindle formation and chromosome segregation, and reduce the oocyte developmental potential (Zhang et al., 2006). High ROS in oocytes may affect the viability and integrity of various organelles and the cytoskeleton, thus impairing their activity, organization and distribution (Kogo et al., 2011). The GSH protects the spindle against oxidative damage and maintains the meiotic spindle morphology (Zuelke et al., 1997). Abnormal mitochondrial metabolism during OS caused defective spindles and misaligned chromosomes in MII oocytes. In addition, our results showed that *in vivo* MII oocytes from insulin-resistant mice displayed a partial premature CG exocytosis (PCE). OS impaired the cortical membrane exocytosis (Bierkamp et al., 2010), which may contribute to a partial premature CG exocytosis in insulin-resistant mice. These results are essential for understanding the detrimental embryo development and increased miscarriage risks in hyperinsulinemic and insulin-resistant individuals (Zhang et al., 2006).

Fully grown oocytes regulate the function of cumulus cells, while nutritional support from cumulus cells is essential for the growth and development of the oocyte (Eppig, 2001). Oocytes utilize glucose poorly as an energy substrate. However, oocyte-derived bone

morphogenetic protein 15 and fibroblast growth factors co-operate to promote glycolysis in cumulus cells (Sugiura *et al.*, 2007). Obesity and hyperinsulinemia significantly affected oocyte quality, which may be associated with relative higher glucose levels through a combination of higher follicular glucose levels and increased activity of glucose transporters within cumulus cells in insulin-resistant mice (Sutton-McDowall *et al.*, 2010). Impacts on the mitochondrial distribution, ATP synthase activities and mitochondrial membrane potential, as well as increased oxidative damage were observed in the type 2 diabetic heart and this may result from the modulation of spatially distinct mitochondrial proteomes (Dabkowski *et al.*, 2010). Next, the interaction of oocytes with cumulus cells insulin-resistant mice needs clarification.

In conclusion, the present study demonstrates that OS occurs in the GV and MII oocytes of insulin-resistant mice, and IR impairs mitochondrial function. Specifically, we firstly reported that IR leads to high energy metabolism with early apoptosis in GV oocytes, which affected oocyte maturation and was associated with poor quality oocytes. Importantly, this work provides new insights into possible treatment options for infertility and PCOS patients with IR, thereby improving their fertility and decreasing the risks of miscarriage.

Acknowledgements

We are grateful to Shi-Wen Li and Ying-Chun Ouyang for their technical assistance and Drs Shu-Tao Qi, Zhao-Jia Ge, Shi-Ming Luo and De-Qiang Miao for insightful suggestions on the manuscript.

Authors' roles

Q.-Y.S. conducted the experiments, researched data, revised the manuscript and obtained funding. X.-H.O. did the experiments, researched data, analyzed data and wrote the manuscript. S.L., Z.-B.W. and L.G. participated in the experiments and contributed to the discussion. H.S. and M.L. revised manuscript. S.-B.C. and X.-W.L. reviewed the manuscript. S.Q., Z.C., Y.H. and F.X. conducted the experiments and reviewed the manuscript.

Funding

This work was supported by the National Basic Research Program of China (2012CB944404, 2011CB944501) and National Natural Science Foundation of China (No. 30930065) to Q.-Y.S.

Conflict of interest

None declared.

References

- Acevedo N, Ding J, Smith GD. Insulin signaling in mouse oocytes. *Biol Reprod* 2007;**77**:872–879.
- Agarwal A, Gupta S, Sharma R. Oxidative stress and its implications in female infertility—a clinician's perspective. *Reprod Biomed Online* 2005; **11**:641–650.
- Agarwal A, Gupta S, Sekhon L, Shah R. Redox considerations in female reproductive function and assisted reproduction: from molecular mechanisms to health implications. *Antioxid Redox Signal* 2008; **10**:1375–1403.
- Bierkamp C, Luxey M, Metchat A, Audouard C, Dumollard R, Christians E. Lack of maternal Heat Shock Factor 1 results in multiple cellular and developmental defects, including mitochondrial damage and altered redox homeostasis, and leads to reduced survival of mammalian oocytes and embryos. *Dev Biol* 2010;**339**:338–353.
- Boirie Y. Insulin regulation of mitochondrial proteins and oxidative phosphorylation in human muscle. *Trends Endocrinol Metab* 2003; **14**:393–394.
- Boldogh IR, Pon LA. Mitochondria on the move. *Trends Cell Biol* 2007; **17**:502–510.
- Brevini TA, Vassena R, Francisci C, Gandolfi F. Role of adenosine triphosphate, active mitochondria, and microtubules in the acquisition of developmental competence of parthenogenetically activated pig oocytes. *Biol Reprod* 2005;**72**:1218–1223.
- Brothers KJ, Wu S, DiVall SA, Messmer MR, Kahn CR, Miller RS, Radovick S, Wondisford FE, Wolfe A. Rescue of obesity-induced infertility in female mice due to a pituitary-specific knockout of the insulin receptor. *Cell Metab* 2010;**12**:295–305.
- Butler ST, Pelton SH, Bulter WR. Insulin increases 17 beta-estradiol production by the dominant follicle of the first postpartum follicle wave in dairy cows. *Reproduction* 2004;**127**:537–545.
- Cano F, Garcia-Velasco JA, Millet A, Remohi J, Simon C, Pellicer A. Oocyte quality in polycystic ovaries revisited: identification of a particular subgroup of women. *J Assist Reprod Genet* 1997;**14**:254–261.
- Cao L, Shitara H, Horii T, Nagao Y, Imai H, Abe K, Hara T, Hayashi J, Yonekawa H. The mitochondrial bottleneck occurs without reduction of mtDNA content in female mouse germ cells. *Nat Genet* 2007;**39**:386–390.
- Carriere A, Galinier A, Fernandez Y, Carmona MC, Penicaud L, Casteilla L. Physiological and physiopathological consequences of mitochondrial reactive oxygen species. *Med Sci (Paris)* 2006;**22**:47–53.
- Chen Q, Vazquez EJ, Moghaddas S, Hoppel CL, Lesnfsky EJ. Production of reactive oxygen species by mitochondria: central role of complex III. *J Biol Chem* 2003;**278**:36027–36031.
- Chen K, Zhang Q, Wang J, Liu F, Mi M, Xu H, Chen F, Zeng K. Taurine protects transformed rat retinal ganglion cells from hypoxia-induced apoptosis by preventing mitochondrial dysfunction. *Brain Res* 2009; **1279**:131–138.
- Combelles CM, Albertini DF. Assessment of oocyte quality following repeated gonadotropin stimulation in the mouse. *Biol Reprod* 2003; **68**:812–821.
- Cummins JM. The role of maternal mitochondria during oogenesis, fertilization and embryogenesis. *Reprod Biomed Online* 2002;**4**:176–182.
- Dabkowski ER, Baseler WA, Williamson CL, Powell M, Razunguzwa TT, Frisbee JC, Hollander JM. Mitochondrial dysfunction in the type 2 diabetic heart is associated with alterations in spatially distinct mitochondrial proteomes. *Am J Physiol Heart Circ Physiol* 2010;**299**:H529–H540.
- Dale PO, Tanbo T, Haug E, Abyholm T. The impact of insulin resistance on the outcome of ovulation induction with low-dose follicle stimulating hormone in women with polycystic ovary syndrome. *Hum Reprod* 1998;**13**:567–570.
- Deneke SM, Fanburg BL. Regulation of cellular glutathione. *Am J Physiol* 1989;**257**:L163–L173.
- Djurovic S, Schjetlein R, Wisloff F, Haugen G, Berg K. Increased levels of intercellular adhesion molecules and vascular cell adhesion molecules in pre-eclampsia. *Br J Obstet Gynaecol* 1997;**104**:466–470.
- Eppig JJ. Oocyte control of ovarian follicular development and function in mammals. *Reproduction* 2001;**122**:829–838.
- Evans JL, Goldfine ID, Maddux BA, Grodsky GM. Oxidative stress and stress-activated signaling pathways: a unifying hypothesis of type 2 diabetes. *Endocr Rev* 2002;**23**:599–622.

- Goud AP, Goud PT, Diamond MP, Gonik B, Abu-Soud HM. Reactive oxygen species and oocyte aging: role of superoxide, hydrogen peroxide, and hypochlorous acid. *Free Radic Biol Med* 2008; **44**:1295–1304.
- Gualtieri R, Iaccarino M, Mollo V, Prisco M, Iaccarino S, Talevi R. Slow cooling of human oocytes: ultrastructural injuries and apoptotic status. *Fertil Steril* 2009; **91**:1023–1034.
- Harvey AJ, Kind KL, Thompson JG. REDOX regulation of early embryo development. *Reproduction* 2002; **123**:479–486.
- Homburg R. Should patients with polycystic ovarian syndrome be treated with metformin? A note of cautious optimism. *Hum Reprod* 2002; **17**:853–856.
- Igosheva N, Abramov AY, Poston L, Eckert JJ, Fleming TP, Duchon MR, McConnell J. Maternal diet-induced obesity alters mitochondrial activity and redox status in mouse oocytes and zygotes. *PLoS ONE* 2010; **5**:e10074.
- Ihnat MA, Thorpe JE, Kamat CD, Szabo C, Green DE, Warnke LA, Lacza Z, Cselenyak A, Ross K, Shakir S et al. Reactive oxygen species mediate a cellular 'memory' of high glucose stress signalling. *Diabetologia* 2007; **50**:1523–1531.
- Jozwik M, Wolczynski S, Szamatowicz M. Oxidative stress markers in preovulatory follicular fluid in humans. *Mol Hum Reprod* 1999; **5**:409–413.
- Kim JA, Wei Y, Sowers JR. Role of mitochondrial dysfunction in insulin resistance. *Circ Res* 2008; **102**:401–414.
- Kogo N, Tazaki A, Kashino Y, Morichika K, Orii H, Mochii M, Watanabe K. Germ-line mitochondria exhibit suppressed respiratory activity to support their accurate transmission to the next generation. *Dev Biol* 2011; **349**:462–469.
- Kovacs G, Wood C. The current status of polycystic ovary syndrome. *Aust N Z J Obstet Gynaecol* 2001; **41**:65–68.
- Krieger-Brauer HI, Medda PK, Kather H. Insulin-induced activation of NADPH-dependent H₂O₂ generation in human adipocyte plasma membranes is mediated by Galphai2. *J Biol Chem* 1997; **15**:10135–10143.
- Lima MH, Souza LC, Caperuto LC, Bevilacqua E, Gasparetti AL, Zanuto R, Saad MJ, Carvalho CR. Up-regulation of the phosphatidylinositol 3-kinase/protein kinase B pathway in the ovary of rats by chronic treatment with hCG and insulin. *J Endocrinol* 2006; **190**:451–459.
- Lintsen AM, Pasker-de Jong PC, de Boer EJ, Burger CW, Jansen CA, Braat DD, van Leeuwen FE. Effects of subfertility cause, smoking and body weight on the success rate of IVF. *Hum Reprod* 2005; **20**:1867–1875.
- Liu L, Trimarchi JR, Keefe DL. Involvement of mitochondria in oxidative stress-induced cell death in mouse zygotes. *Biol Reprod* 2000; **62**:1745–1753.
- Luderer U, Kavanagh TJ, White CC, Faustman EM. Gonadotropin regulation of glutathione synthesis in the rat ovary. *Reprod Toxicol* 2001; **15**:495–504.
- Ludwig M, Finas DF, al-Hasani S, Diedrich K, Ortmann O. Oocyte quality and treatment outcome in intracytoplasmic sperm injection cycles of polycystic ovarian syndrome patients. *Hum Reprod* 1999; **14**:354–358.
- Madsen-Bouterse SA, Zhong Q, Mohammad G, Ho YS, Kowluru RA. Oxidative damage of mitochondrial DNA in diabetes and its protection by manganese superoxide dismutase. *Free Radic Res* 2010; **44**:313–321.
- Martin SJ, Reutelingsperger CP, McGahon AJ, Rader JA, van Schie RC, LaFace DM, Green DR. Early redistribution of plasma membrane phosphatidylserine is a general feature of apoptosis regardless of the initiating stimulus: inhibition by overexpression of Bcl-2 and Abl. *J Exp Med* 1995; **182**:1545–1556.
- Mtango NR, Potireddy S, Latham KE. Oocyte quality and maternal control of development. *Int Rev Cell Mol Biol* 2008; **268**:223–290.
- Nagai S, Mabuchi T, Hirata S, Shoda T, Kasai T, Yokota S, Shitara H, Yonekawa H, Hoshi K. Oocyte mitochondria: strategies to improve embryogenesis. *Hum Cell* 2004; **17**:195–201.
- Nagano M, Katagiri S, Takahashi Y. ATP content and maturational/developmental ability of bovine oocytes with various cytoplasmic morphologies. *Zygote* 2006; **14**:299–304.
- Perez GI, Acton BM, Jurisicova A, Perkins GA, White A, Brown J, Trbovich AM, Kim MR, Fissore R, Xu J et al. Genetic variance modifies apoptosis susceptibility in mature oocytes via alterations in DNA repair capacity and mitochondrial ultrastructure. *Cell Death Differ* 2007; **14**:524–533.
- Petersen KF, Dufour S, Befroy D, Garcia R, Shulman GI. Impaired mitochondrial activity in the insulin-resistant offspring of patients with type 2 diabetes. *N Engl J Med* 2004; **350**:664–671.
- Poretsky L, Clemons J, Bogovich K. Hyperinsulinemia and human chorionic gonadotropin synergistically promote the growth of ovarian follicular cysts in rats. *Metabolism* 1992; **41**:903–910.
- Qian H, Chen W, Li J, Wang J, Zhou Z, Liu W, Fu Z. The effect of exogenous nitric oxide on alleviating herbicide damage in *Chlorella vulgaris*. *Aquat Toxicol* 2009; **92**:250–257.
- Ratchford AM, Chang AS, Chi MM, Sheridan R, Moley KH. Maternal diabetes adversely affects AMP-activated protein kinase activity and cellular metabolism in murine oocytes. *Am J Physiol Endocrinol Metab* 2007; **293**:E1198–E1206.
- Reers M, Smiley ST, Mottola-Hartshorn C, Chen A, Lin M, Chen LB. Mitochondrial membrane potential monitored by JC-1 dye. *Methods Enzymol* 1995; **260**:406–417.
- Robker RL, Akison LK, Bennett BD, Thrupp PN, Chura LR, Russell DL, Lane M, Norman RJ. Obese women exhibit differences in ovarian metabolites, hormones, and gene expression compared with moderate-weight women. *J Clin Endocrinol Metab* 2009; **94**:1533–1540.
- Ross PJ, Yabuuchi A, Cibelli JB. Oocyte spontaneous activation in different rat strains. *Cloning Stem Cells* 2006; **8**:275–282.
- Samoto T, Maruo T, Ladines-Llave CA, Matsuo H, Deguchi J, Barnea ER, Mochizuki M. Insulin receptor expression in follicular and stromal compartments of the human ovary over the course of follicular growth, regression and atresia. *Endocr J* 1993; **40**:715–726.
- Shitara H, Kaneda H, Sato A, Inoue K, Ogura A, Yonekawa H, Hayashi JJ. Selective and continuous elimination of mitochondria microinjected into mouse eggs from spermatids, but not from liver cells, occurs throughout embryogenesis. *Genetics* 2000; **156**:1277–1284.
- Sleigh A, Raymond-Barker P, Thackray K, Porter D, Hatunic M, Vottero A, Burren C, Mitchell C, McIntyre M, Brage S et al. Mitochondrial dysfunction in patients with primary congenital insulin resistance. *J Clin Invest* 2011; **121**:2457–2461.
- Spikings EC, Alderson J, St John JC. Regulated mitochondrial DNA replication during oocyte maturation is essential for successful porcine embryonic development. *Biol Reprod* 2007; **76**:327–335.
- Stump CS, Short KR, Bigelow ML, Schimke JM, Nair KS. Effect of insulin on human skeletal muscle mitochondrial ATP production, protein synthesis, and mRNA transcripts. *Proc Natl Acad Sci USA* 2003; **100**:7996–8001.
- Sugiura K, Su YQ, Diaz FJ, Pangas SA, Sharma S, Wigglesworth K, O'Brien MJ, Matzuk MM, Shimasaki S, Eppig JJ. Oocyte-derived BMP15 and FGFs cooperate to promote glycolysis in cumulus cells. *Development* 2007; **134**:2593–2603.
- Sutton-McDowall ML, Gilchrist RB, Thompson JG. The pivotal role of glucose metabolism in determining oocyte developmental competence. *Reproduction* 2010; **139**:685–695.

- Svendsen PF, Nilas L, Norgaard K, Jensen JE, Madsbad S. Obesity, body composition and metabolic disturbances in polycystic ovary syndrome. *Hum Reprod* 2008;**23**:2113–2121.
- Thouas GA, Trounson AO, Wolvetang EJ, Jones GM. Mitochondrial dysfunction in mouse oocytes results in preimplantation embryo arrest in vitro. *Biol Reprod* 2004;**71**:1936–1942.
- Tripathi A, Khatun S, Pandey AN, Mishra SK, Chaube R, Shrivastav TG, Chaube SK. Intracellular levels of hydrogen peroxide and nitric oxide in oocytes at various stages of meiotic cell cycle and apoptosis. *Free Radic Res* 2009;**43**:287–294.
- Tsai-Turton M, Luong BT, Tan Y, Luderer U. Cyclophosphamide-induced apoptosis in COV434 human granulosa cells involves oxidative stress and glutathione depletion. *Toxicol Sci* 2007;**98**:216–230.
- Valko M, Leibfritz D, Moncol J, Cronin MT, Mazur M, Telser J. Free radicals and antioxidants in normal physiological functions and human disease. *Int J Biochem Cell Biol* 2007;**39**:44–84.
- Van Blerkom J. Mitochondrial function in the human oocyte and embryo and their role in developmental competence. *Mitochondrion* 2011;**11**:797–813.
- Van Blerkom J, Davis P, Alexander S. Inner mitochondrial membrane potential (DeltaPsi_m), cytoplasmic ATP content and free Ca²⁺ levels in metaphase II mouse oocytes. *Hum Reprod* 2003;**18**:2429–2440.
- Van Blerkom J, Cox H, Davis P. Regulatory roles for mitochondria in the peri-implantation mouse blastocyst: possible origins and developmental significance of differential DeltaPsi_m. *Reproduction* 2006;**131**:961–976.
- Victor VM, Rocha M, Banuls C, Sanchez-Serrano M, Sola E, Gomez M, Hernandez-Mijares A. Mitochondrial complex I impairment in leukocytes from polycystic ovary syndrome patients with insulin resistance. *J Clin Endocrinol Metab* 2009;**94**:3505–3512.
- Vlaisavljevic V, Kovac V, Sajko MC. Impact of insulin resistance on the developmental potential of immature oocytes retrieved from human chorionic gonadotropin-primed women with polycystic ovary syndrome undergoing in vitro maturation. *Fertil Steril* 2009;**91**:957–959.
- Wai T, Ao A, Zhang X, Cyr D, Dufort D, Shoubridge EA. The role of mitochondrial DNA copy number in mammalian fertility. *Biol Reprod* 2010;**83**:52–62.
- Wallace DC. The epigenome and the mitochondrion: bioenergetics and the environment [corrected]. *Genes Dev* 2010;**24**:1571–1573.
- Wang Q, Ratchford AM, Chi MM, Schoeller E, Frolova A, Schedl T, Moley KH. Maternal diabetes causes mitochondrial dysfunction and meiotic defects in murine oocytes. *Mol Endocrinol* 2009;**23**:1603–1612.
- Yoo JG, Smith LC. Extracellular calcium induces activation of Ca(2+)/calmodulin-dependent protein kinase II and mediates spontaneous activation in rat oocytes. *Biochem Biophys Res Commun* 2007;**359**:854–859.
- Zhang X, Wu XQ, Lu S, Guo YL, Ma X. Deficit of mitochondria-derived ATP during oxidative stress impairs mouse MII oocyte spindles. *Cell Res* 2006;**16**:841–850.
- Zuelke KA, Jones DP, Perreault SD. Glutathione oxidation is associated with altered microtubule function and disrupted fertilization in mature hamster oocytes. *Biol Reprod* 1997;**57**:1413–1419.